

Chemistry of Iron Thiolate Complexes with CN⁻ and CO. Models for the [Fe(CO)(CN)₂] Structural Unit in Ni–Fe Hydrogenase Enzymes

Hua-Fen Hsu and Stephen A. Koch*

Department of Chemistry
State University of New York at Stony Brook
Stony Brook, New York 11794-3400

Codrina V. Popescu and Eckard Münck*

Department of Chemistry, Carnegie Mellon University
Pittsburgh, Pennsylvania 15213

Received April 10, 1997

A combination of protein crystallography and vibrational spectroscopy has established a [(Cys-S)₂Ni(μ₂-S-Cys)₂Fe(CO)(CN)₂] binuclear unit as the active site of the Ni–Fe hydrogenase enzymes.^{1–3} Previously, neither CO nor CN⁻ had been found as a native ligand in a metalloprotein. In addition to the two bridging cysteines, there is crystallographic evidence for a light atom (X) bridging the two metal centers.¹ Recent FTIR studies indicate that the various redox states of the enzyme give characteristic shifts in the CO and CN stretching frequencies.^{1a,2} The shifts in the stretching frequencies (CO 1950–1898 cm⁻¹; CN 2093–2044 cm⁻¹) could reflect (a) changes in oxidation states of the iron center, (b) changes in electron density on the iron center caused by changes in the redox state of the nickel center and/or (c) changes in the ligation of the iron center (i.e., the X ligand). Vibrational bands consistent with CO and CN⁻ or similar multiply bonded diatomics have also been found in iron-only hydrogenases.^{2b} An [Fe^{II}–CN–Ni] assembly has been proposed for cyanide inhibited carbon monoxide dehydrogenase.⁴ As has been frequently the case in the history of bioinorganic chemistry, a metalloprotein center has been discovered with no counterpart among the synthetic coordination complexes. The coordination chemistry of iron(II) complexes with CN⁻ and CO as ligands is severely limited.⁵ We report the synthesis and characterization of the first iron(II) thiolate complex with CN⁻ and CO ligands and its reversible oxidation in solution to an Fe(III) species.

The reaction of 3 equiv of NaCN with FeCl₂·4H₂O and Li₃PS₃⁶ in MeOH followed by the addition of Me₃BzNBr gives [Me₃BzN]₂[Fe^{II}(PS₃)(CN)] (HOMe) (**1**).⁷ A related synthesis in which the Fe(II) species is oxidized with air gives an Fe(III) analog of **1**, [Li(DMF)₃][Fe^{III}(PS₃*)₂(CN)] (**2**).^{6,8} Both **1**⁹ (Figure 1) and **2**^{10,11} have trigonal bipyramidal structures in which the CN⁻ is *trans* to the phosphorus. In **1**, there is a hydrogen-bonding interaction between a MeOH and the N of the CN⁻. Compound **2** exhibits a crystallographically imposed

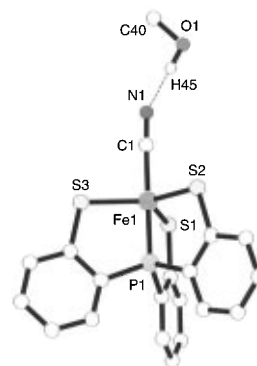


Figure 1. Structural diagram of [Fe^{II}(PS₃)(CN)]²⁻ (HOCH₃) (**1**). Selected bond distances (Å) and angles (deg): Fe–S1 2.306(1); Fe–S2 2.279(1); Fe–S3 2.278(1); Fe–C1 1.947(4); Fe–P1 2.142(1); C1–N1 1.156(4); S1–Fe–S2 117.25(5); S1–Fe–S3 119.11(25); S2–Fe–S3 122.69(5); S1–Fe–P1 86.73(4); S2–Fe–P1 86.91(5); S3–Fe–P1 86.61(5); S1–Fe–C1 93.8(1); S2–Fe–C1 92.5(1); S3–Fe–C1 93.5(1); P1–Fe–C37 179.3(1).

C₃ symmetry axis. The lithium cation is coordinated to the N atom of the CN⁻ ligand and to three DMF molecules. Compounds **1** and **2**, which are the first crystallographically characterized iron thiolate cyanide complexes, are structurally similar to the previously reported [Et₄N][Fe^{II}(PS₃*)₂(CO)] (**3**).¹² As was the case for **3**, compound **1** contains an intermediate spin ferrous ion (*S* = 1, ground state), consistent with the trigonal bipyramidal symmetry, which does not permit an *S* = 0 ground state.¹² Compound **2** has a magnetic moment (μ_{eff} = 1.82 μ_{B}) consistent with a *S* = 1/2 ground state. There is a large difference in the Fe–S_{ave} for **1** (2.29(2) Å) and **2** (2.167(1) Å) but no significant difference in the Fe–CN distance (1.947(4) Å in **1**; 1.938(7) Å in **2**). The CN stretching frequency shifts to lower energy and to higher intensity upon reduction from Fe(III) (2094 cm⁻¹) to Fe(II) (2070 cm⁻¹).¹³ Cyclic voltammetric and controlled potential electrolysis studies indicate that **1** and **2** are members of a three-membered electron transfer series which includes the Fe(IV) analog. The midpoint potential of the Fe^{4+/3+} couple (for **1**) is at 0.390 V, whereas that of the Fe^{3+/2+} couple is at –0.588 V (vs SCE).

At 25 °C, reaction of **1** with CO (1 atm) in methanol gives [Ph₄P]₂[Fe^{II}(PS₃)(CO)(CN)] (**4**) in 50% yield.¹⁴ The complex crystallizes with the CO and CN⁻ ligands lying on a crystallographically imposed plane of symmetry (Figure 2).¹⁵ The CO and CN⁻ ligands are easily distinguished in the X-ray structure with the CN⁻ ligand remaining *trans* to the phosphorus and the CO ligand adding in the plane of the three thiolate donors.

(1) (a) Volbeda, A.; Garcin, E.; Piras, C.; de Lacey, A. L.; Fernandez, V. M.; Hatchikian, E. C.; Frey, M.; Fontecilla-Camps, J. C. *J. Am. Chem. Soc.* **1996**, *118*, 12989–12996. (b) Fontecilla-Camps, J. C. *J. Biol. Inorg. Chem.* **1996**, *1*, 91–88. (c) Volbeda, A.; Charon, M.-H.; Piras, C.; Hatchikian, E. C.; Frey, M.; Fontecilla-Camps, J. C. *Nature (London)* **1995**, *373*, 580–587.

(2) (a) Happe, R. P.; Roseboom, W.; Pierik, A. J.; Albracht, S. P. J.; Bagley, K. A. *Nature* **1997**, *385*, 126. (b) van der Spek, T. M.; Arendsen, A. F.; Happe, R. P.; Yun, S.; Bagley, K. A.; Stufkens, D. J.; Hagen, W. R.; Albracht, S. P. J. *Eur. J. Biochem.* **1996**, *237*, 629–634. (c) Bagley, K. A.; Van Garderen, C. J.; Chen, M.; Duin, E. C.; Albracht, S. P. J.; Woodruff, W. H. *Biochemistry* **1994**, *33*, 9229–9236. (d) Bagley, K. A.; Duin, E. C.; Roseboom, W.; Albracht, S. P. J.; Woodruff, W. H. *Biochemistry* **1995**, *34*, 5527–5535.

(3) Albracht, S. P. J. *Biochim. Biophys. Acta* **1994**, *1188*, 167–204.

(4) Qiu, D.; Kumar, M.; Ragsdale, S. W.; Spiro, T. G. *J. Am. Chem. Soc.* **1996**, *118*, 10429–10435.

(5) (a) Sharpe, A. G. *The Chemistry of Cyano Complexes of the Transition Metals*; Academic Press: New York, 1976. (b) Dunbar, K. R.; Heintz, R. A. *Prog. Inorg. Chem.* **1997**, *45*, 283 and references therein.

(6) (PS₃)H₃ = tris(2-phenylthiol)phosphine; (PS₃*)₃ = tris(3-phenyl-2-thiophenyl)phosphine.

(7) Compound **1**: ¹H NMR (DMSO-*d*₆) –30.90 (3H), –9.04 (3H), 3.12 (18H), 3.56 (3H), 4.07 (3H), 4.48 (4H), 7.51 (10H); UV–vis in DMF, λ (ϵ_{M}) 1064 (5.02 × 10³), 527 (2.81 × 10³), 413 (3.95 × 10³), 334 (1.36 × 10⁴) nm; (μ_{eff} = 2.63 μ_{B}).

(8) Electronic spectrum of **2** in DMF, λ (ϵ_{M}) 792 (3.87 × 10³), 634 (3.17 × 10³), 486 (4.64 × 10³), 422 (8.06 × 10³), 348 nm (1.75 × 10⁴).

(9) Crystal data for **1** (FePS₃N₃O₃C₄₀H₄₈): triclinic, P1 (No. 2), *a* = 9.811(1) Å, *b* = 14.771(1) Å, *c* = 15.089(2) Å, α = 109.010(8)°, β = 106.329(9)°, γ = 90.024(9)°. *V* = 1974.5(4) Å³, *Z* = 2. A total of 4110 unique reflections with *I* > 3 σ (*I*) were refined to *R* = 0.043 and *R*_w = 0.033.

(10) Crystal data for **2** (FePS₃N₄O₃C₄₉H₄₅Li): trigonal, P3c1 (No. 165), *a* = *b* = 14.9382(9) Å, *c* = 25.609(4) Å, *V* = 4949.1(4) Å³, *Z* = 4. A total of 1499 unique reflections with *I* > 3 σ (*I*) were refined to *R* = 0.044 and *R*_w = 0.048.

(11) [Li(DMF)₃][Fe^{III}(PS₃*)₂(CN)] (**2**). Selected bond distances (Å) and angles (deg): Fe–S1 2.167(1); Fe–P1 2.141(2); Fe–C13 1.938(7); C13–N1 1.143(8); Li1–N1 2.03(1); S1–Fe–S1' 119.869(5); S1–Fe–P1 87.92(4); S1–Fe–C13 92.08(4); P1–Fe–C13 180.00.

(12) Nguyen, D. H.; Hsu, H.-F.; Millar, M.; Koch, S. A.; Achim, C.; Bominaar, E. L.; Münck, E. *J. Am. Chem. Soc.* **1996**, *118*, 8963–8964.

(13) Swanson, B. I.; Hamburg, S. I.; Ryan, R. R. *Inorg. Chem.* **1974**, *13*, 1685–1687.

(14) Electronic spectrum of **4** in DMF, λ (ϵ_{M}) 736 (2.70 × 10²), 511 (1.62 × 10³).

(15) Crystal data for **4** (FeP₃S₃N₃O₃C₇₀H₆₀): monoclinic, P2₁/m (No. 11), *a* = 10.710(3) Å, *b* = 22.845(2) Å, *c* = 12.307(3) Å, β = 101.09(1)°, *V* = 2955(1) Å³, *Z* = 2. A total of 3068 unique reflections with *I* > 3 σ (*I*) were refined to *R* = 0.048 and *R*_w = 0.039.

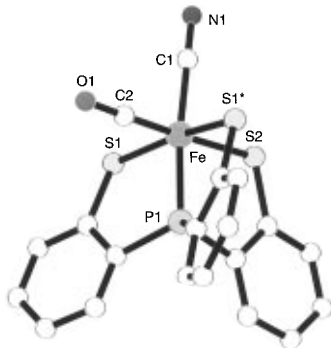


Figure 2. Structural diagram of $[\text{Fe}^{\text{II}}(\text{PS3})(\text{CO})(\text{CN})]^{2-}$ (**4**). Selected bond distances (\AA) and angles (deg): Fe–S1 2.319(1); Fe–S2 2.325(2); Fe–C1 1.950(8); Fe–C2 1.710(8); Fe–P1 2.152(2); C1–N1 1.154(8); C2–O1 1.173(7); S1–Fe–S2 94.39(4); S1–Fe–S1* 166.13(8); S1–Fe–C1 95.71(5); S1–Fe–C2 85.83(5); S1–Fe–P1 84.91(5); S2–Fe–P1 86.60(9); S2–Fe–C1 85.2(2); S2–Fe–C2 177.7(3); P1–Fe–C1 171.8(2); C1–Fe–C2 92.5(3).

The Fe–C(N) distance (1.950(8) \AA) is similar to that in **1**. The Fe–C(O) distance (1.710(8) \AA) lies at the short end of the range of Fe–C distances (1.70–1.80 \AA) found for six-coordinate Fe(II) monocarbonyl complexes.¹⁶ The only other crystallographically characterized monomeric complex of iron with CN^- and CO ligands is the Fe(0) compound, $[\text{PPN}][\text{Fe}(\text{CO})_4(\text{CN})]$.¹⁷ Among non-structurally characterized complexes, $[\text{CpFe}(\text{CO})(\text{CN})_2]^{1-}$ and $[\text{Fe}(\text{CO})(\text{CN})_5]^{3-}$ are the most relevant.^{18,19}

The IR spectrum of **4** (DMF) displays sharp absorption bands at 2079 and 1904 cm^{-1} which are assigned to CN and CO stretches, respectively. The CN stretching frequency is shifted by 9 cm^{-1} to higher frequency compared to that in **1** while the CO stretching frequency is shifted to lower energy by 36 cm^{-1} compared to that in **3**.¹² As is observed for hydrogenase, the CO stretch is more intense than the CN stretch.^{1a,2} Because dilute solutions of **4** show evidence for partial dissociation of the CO ligand, solution spectroscopic and electrochemical studies were performed under a CO atmosphere.

Mössbauer (4.2 K) spectra of polycrystalline **4** are shown in Figure 3. The zero field spectrum (A) exhibits a sharp quadrupole doublet with $\Delta E_{\text{Q}} = 0.91(2)$ mm/s and $\delta = 0.15(1)$ mm/s (with respect to Fe metal, at 298 K). The 8.0 T spectrum of Figure 3B exhibits magnetic splittings entirely attributable to the nuclear Zeeman interaction, i.e., the compound is diamagnetic. Taken together, these data imply that **4** is a low-spin Fe(II) compound. A Mössbauer study²⁰ of the *Chromatium vinosum* Ni–Fe hydrogenase (1 Ni, 12 Fe) has revealed a spectral component with unusually small isomer shift, $\delta \sim 0.05$ –0.15 mm/s. The present study, together with the recent protein IR and X-ray data,^{1,2} suggests that the unusual spectral component should be assigned to the iron of the dinuclear Ni–Fe cluster.²⁰

The electrochemistry of **4** (in DMF) shows a reversible oxidation couple at -0.476 V (vs SCE). The combination of CN^- and CO as ligands does not effect a major shift in the redox potential. For example, **1** and $[(\text{PS3})\text{Fe}^{\text{II}}(\text{N-methylimidazole})]$ show similar potentials. The chemical reversibility of the Fe(III)/Fe(II) couple for **4** was established by controlled potential electrolysis. The CV of the electrochemically gener-

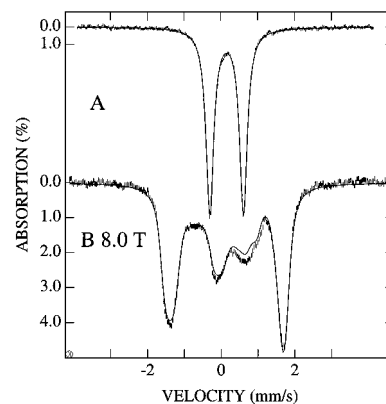


Figure 3. Mössbauer (4.2 K) spectra of polycrystalline **4**, recorded in zero field (A) and an 8.0 T magnetic field, applied parallel to the incident γ -radiation. (B). The solid line in spectrum A is a least-squares fit to the data, while the solid line in spectrum B is a spectral simulation generated with the assumption that the electronic ground state of **4** has $S = 0$; this simulation also shows that $\Delta E_{\text{Q}} < 0$ and $0.4 < \eta < 0.8$.

ated Fe(III) species shows the same reversible Fe(III)/Fe(II) couple as **4**. The infrared spectra of solutions obtained by the chemical oxidation of **4** in DMF with Cp_2FeBF_4 show a CO stretch at 2006 cm^{-1} and a CN stretch at 2108 cm^{-1} . Attempts are underway to isolate and structurally characterize this $\text{Fe}^{\text{III}}(\text{CO})(\text{CN})$ species. $\text{Fe}^{\text{III}}\text{CO}$ species are unusual, with the few previous examples limited to organometallic compounds.^{21,22}

The redox induced shifts in the stretching frequencies of CO (102 cm^{-1}) and CN (29 cm^{-1}) in **4** indicate the magnitude of the shifts that could be expected for a redox change in similar $\text{Fe}(\text{CO})(\text{CN})_2$ centers in the enzymes. The total range of the CO stretching frequency in the various states of Ni–Fe hydrogenases is 50 cm^{-1} , with smaller shifts occurring during individual 1e reductions of the enzyme.^{1a,2} There are only small differences in the CO stretching frequencies in the Ni–A (1944 cm^{-1}), which is the most oxidized form of the enzyme, Ni–C (1950 cm^{-1}), and Ni–R (1936 cm^{-1}), the most reduced form of the enzyme.² The comparison between the redox changes in the IR frequencies in the Ni A/B/C and R states of the Ni–Fe hydrogenases (of the order of 10 cm^{-1} , or less) and those in the present model complex (102 cm^{-1}) suggests that the oxidation state of the Fe in the binuclear site of the enzyme stays unchanged upon oxidation/reduction. The EPR spectra of the Ni–A/B states of hydrogenase showed that there is no paramagnet close to the Ni site, which led to the conclusion that the Fe site is a low-spin iron(II).

The discovery of the $[\text{Fe}(\text{CO})(\text{CN})_2]$ structural unit in hydrogenase enzymes has raised many possibilities as to its function in the activation and/or evolution of H_2 . Attempts to model the $[\text{Fe}(\text{CO})(\text{CN})_2]$ hydrogenase center in more detail are underway in our laboratories.

Acknowledgment. We thank Professor Michelle Millar for stimulating discussion. This research was supported by NIH GM 31849 (S.K.) and NSF MCB 9406274 (E.M.).

Supporting Information Available: Tables of crystallographic parameters, atomic coordinates, thermal parameters, and bond distances and angles for **1**, **2**, and **4** (20 pages). See any current masthead page for ordering and Internet access instructions.

JA971139L

(16) (a) Sellmann, D.; Becker, T.; Knoch, F. *Chem. Eur. J.* **1996**, *2*, 1092–1098 and references therein. (b) Scheidt, W. R.; Haller, K. J.; Fons, M.; Mashiko, T.; Reed, C. A. *Biochemistry* **1981**, *20*, 3653–3657. (c) Busch, D. H.; Zimmer, L. L.; Grzybowski, J. J.; Olszanski, D. J.; Jackels, S. C.; Callahan, R. C.; Christoph, Gary G. *Proc. Natl. Acad. Sci. U.S.A.* **1981**, *78*, 5919–5923.

(17) Coffield, S. A.; Raymond, K. N. *Inorg. Chem.* **1974**, *13*, 770–775.

(18) Coffey, C. E. *J. Inorg. Nucl. Chem.* **1963**, 179–185.

(19) *Gmelin*, **1976**, *36B*, 24–27.

(20) Surerus, K. K.; Chen, M.; van der Zwaan, J. W.; Rusnak, F. M.; Kolk, M.; Duin, E. C.; Albracht, S. P.; Münck, E. *Biochemistry* **1994**, *33*(16), 4980–93.

(21) $\Delta\nu_{\text{CO}}$ $[\text{Fe}^{\text{III}}(\text{CO})-\text{Fe}^{\text{II}}(\text{CO})]$ for previous examples of $\text{Fe}^{\text{III}}\text{CO}$ compounds: $[\text{Cp}^*\text{Fe}(\text{CO})(\text{S}_2\text{CNMe}_2)]^{0/1+}$ (~ 82 cm^{-1});^{22a} $[\text{Cp}^*\text{Fe}(\text{CO})(\eta^1\text{-dppe})(\text{CH}_3)]^{0/1+}$ (50);^{22b} $[\text{Cp}^*\text{Fe}(\text{CO})(\text{PPh}_3)(\text{CH}_3)]^{0/1+}$ (62);^{22c} $\{\text{Cp}^*\text{Fe}(\text{CO})(\text{PPh}_3)_2(\mu\text{-CH}=\text{CHCH}=\text{CH})\}^{0/2+}$ (100).^{22d}

(22) (a) Delville-Desbois, M.-H.; Mross, S.; Astruc, D.; Linares, J.; Varret, F.; Rabaà, H.; Le Beuze, A.; Saillard, J.-Y.; Culp, R. D.; Atwood, D. A.; Cowley, A. H. *J. Am. Chem. Soc.* **1996**, *118*, 4133–4147. (b) Morrow, J.; Catheline, D.; Desbois, M.-H.; Manriquez, J.-M.; Ruiz, J.; Astruc, D. *Organometallics* **1987**, *6*, 2605. (c) Therien, M. J.; Troglor, W. C. *J. Am. Chem. Soc.* **1987**, *109*, 5127–5133. (d) Etzenhouser, B. A.; Cavanaugh, M. D.; Spurgeon, H. N.; Sponsler, M. B. *J. Am. Chem. Soc.* **1994**, 2221–2222.